Chemistry, Physics and Technology of Surface. 2017. V. 8. N 1. P. 98-103

UDC 546.05+53.06 doi: 10.15407/hftp08.01.098

S.L. Prokopenko, G.M. Gunja, S.M. Makhno, P.P. Gorbyk

ROOM-TEMPERATURE NH_3 GAS SENSORS BASED ON HETEROSTRUCTURES PbS/CdS

Chuiko Institute of Surface Chemistry of National Academy of Sciences of Ukraine
17 General Naumov Str., Kyiv, 03164, Ukraine, E-mail: sprokop@yandex.ua

In order to develop sensors capable to detect harmful gases at the ambient temperature, the semiconductor heterostructure PbS/CdS has been synthesized. Formation of CdS nanorods was conducted in the presence of ethylenediamine. An ion-exchange method was used to deposit PbS nanoparticles over the CdS nanorods to produce a large area of the surface heterojunction. Series of samples of with variation in the PbS amount on the CdS surface (from 2.5 to 20 mol. %) was obtained. Surface morphology, optical properties and performance characteristics of the PbS/CdS heterostructure gas sensors were studied. The sample performance characteristics were measured by means of change in electric resistance of sensor due to reaction between the surface of material and NH_3 in saturated vapours of ammonia. The gas sensor based on the PbS/CdS heterostructures have shorter response and recovery time compared to a sensor based on the CdS solely. It has been shown that with increase in amount of PbS on the CdS surface from 2.5 to 20 mol. % the sensor response rate becomes 1.7 times greater.

Keywords: *sensor, PbS/CdS heterostructures, ammonia, nanowires*

INTRODUTION

Ammonia plays a vital role in all forms of life and it is the second most widely used chemical in the world [1]. Natural ammonia level present in the atmosphere is low (1–5 ppb). The lower limit of human NH_3 perception by smell is tabulated to be around 25 ppm. It is acutely toxic if inhaled above the moderate quantity. The search for novel and more effective sensors for monitoring of ammonia concentrations in air is of great interest in many fields, including the environmental monitoring, the automotive exhaust detection, and in chemical and medical industries in general [2–5]. However, the high cost of the classical analytical instruments (spectroscopic gas sensor, optical gas sensor, mass chromatography, mass spectrograph, etc.) in monitoring systems limits the control of the air quality.

Alternatively, semiconducting nanomaterials have attracted a considerable interest due to their high sensitivity, selectivity, and short response time. In addition, they have low power consumption, lightweight; possesses a simplicity in operation and a low maintenance cost that is highly attractive for portable applications. One of the mostly used sensing mechanisms for detection of the NH_3 is based on resistive sensors made of various metal oxide semiconductors [6, 7].

In the present study, PbS nanoparticles were deposited over the surface of CdS nanorods at room temperature (25 °C) via straightforward and non-expensive chemical route. The *p*-PbS/*n*-CdS system was applied successfully in NH_3 detection at the ambient conditions.

EXPERIMENTAL DETAILS

CdS nanorods were synthesized through co-crystallization of 0.004 M $Cd(NO_3)_2 \cdot 4H_2O$ (analytical grade) and 0.008 M thiourea (analytical grade) from ethylenediamine ($C_2H_4(NH_2)_2$, analytical grade) (30 ml) at 393 K. After cooling to the ambient temperature, the obtained precipitate was washed with an excess of distilled water, centrifuged and dried at 330 K. Formation of CdS nanorods in ethylenediamine was carried out according to the following equations:

$$n\mathrm{Cd}^{2+} + 2n(\mathrm{EDA}) \leftrightarrow n[\mathrm{Cd(EDA)_2}]^{2+} \quad (1)$$

$$n[\mathrm{Cd(EDA)_2}]^{2+} + n\mathrm{S}^{2-} \xleftrightarrow{EDA} (\mathrm{CdS})_n \ . \quad (2)$$

Cd^{2+} ions from the cadmium nitrate solution react with ethylenediamine ligands forming a relatively stable complex (Eq. 1), which under synthesis conditions promotes a crystal growth (Eq. 2) into a rod-like structure [8].

PbS/CdS heterostructures were obtained via conventional ion-exchange method according to the Eq. 3. In order to form PbS nanoparticles on the surface of CdS nanorods at a different Cd/Pb ratio, the lead acetate solution was added to the CdS nanorods dispersion. CdS/PbS semiconductor nanorods were formed via process when Pb^{2+} ions displace Cd-ions in Cd-S bonds on the surface of CdS nanorods (Eq. 3), even the PbS has a different crystalline structure from that of CdS [9, 10].

$$Pb^{2+} + CdS \rightarrow Cd^{2+} + PbS + \Delta G \qquad (3)$$

where ΔG, the Gibbs free energy of the reaction, equal to –4.618 kJ/mol, which makes the ion exchange possible. Previously [11] was shown that an increase in the Pb-ions concentration leads to increase in the PbS shell due to Pb^{2+} ions diffusion into the CdS nanorod bulk. Samples were named accordingly to the percentage content of the lead ions in the semiconductor.

Crystalline structures of obtained samples were determined using X-ray analysis (DRON-4-07, Lomo, USSR) in the emission of copper cathode with nickel filter in Bragg–Brentano geometry. Diffuse reflectance spectra were recorded using a Lambda-35 spectrophotometer (Perkin-Elmer). Electrical properties were measured on a Solortron SI 1271 potentiostat (Solortron analytical, UK) at the 500 mV. Morphology of samples was studied using a TEM (Transmission Electron Microscope) JEOL JEM-2100F.

For gas sensing purposes, the PbS/CdS nanopowder, obtained as described earlier, was mixed with a suitable amount of adhesive and then ground into a paste. In order to compose the experimental NH_3 sensor, a fiberglass plate was coated with the fresh semiconductor paste using a small brush to form a thick film between two parallel gold electrodes. The NH_3 sensing measurements were carried out in saturated vapors of ammonia.

RESULTS AND DISCUSSION

X-ray diffraction patterns of PbS/CdS heterostructures contain three most intense peaks at 26.7, 43.9 and 51.9° 2Θ, which correspond to (002), (110) and (112) planes of hexagonal CdS (JCPDS 75-1545) and four peaks at 26, 30.1, 43 and 51° 2Θ of the (111), (200), (220) and (311) cubic planes of the PbS (JCPDS 78-1054) respectively (Fig. 1 *a*).

TEM image of the CdS shows a nanorod bundles with an average length of 150–200 nm and a diameter approximately of 20 nm for an individual rod (Fig. 1 *b*).

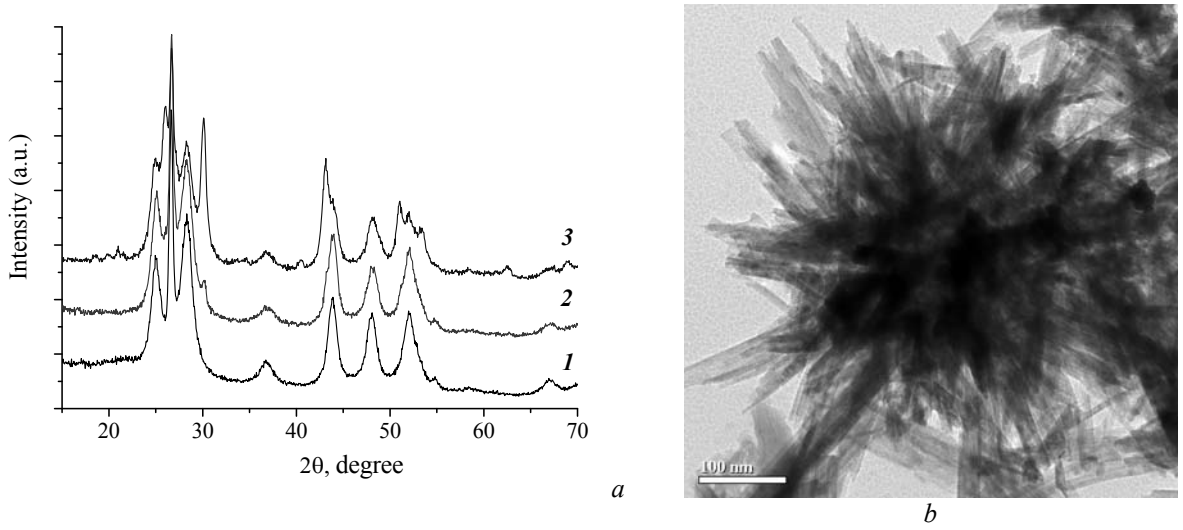

a *b*

Fig. 1. *a* – X-ray diffraction patterns of nanorods and heterostructures: *1* – CdS, *2* – 2.5 % PbS/CdS, *3* – 20 %PbS/CdS; *b* – TEM image of CdS nanowires

UV-Vis spectra of the synthesized samples of CdS and PbS/CdS are shown in Fig. 2 *a*. Nanorods of pristine CdS obtained under experimental conditions have a band gap energy of 2.4 eV (Eq. 4). PbS/CdS heterostructures exhibit a higher absorption than the initial sample and with growth in the Pb content, the absorption band extends to the wavelength range 550 to 1100 nm.

The band gap E_g was calculated from the following equation:

$$(\alpha h\nu)^n = A(h\nu - E_g) \quad (4)$$

where hν is the photon energy, α is the absorption coefficient, A is a constant characteristic of the material, E_g is the band gap, and n depends of the type of transition. If the value of n = 1/2, 2, 3/2 and 3, the band gap is of: allowed direct, allowed indirect, forbidden direct and forbidden indirect type, respectively. The curve of calculated $(\alpha h\nu)^2$ versus hν for 15 % PbS/CdS sample is shown in Fig. 2 *b*. The value of hν extrapolated to α = 0 gives the absorption band gap energy. The curve in Fig. 2 *b* can be linearly fitted into two lines with intercepts at 2.25 and 1.38 eV. The band gap values for 15 % PbS/CdS sample are higher than those for CdS and PbS (2.25 eV [12] and 0.41 eV [13], respectively), indicating that the sizes of CdS and PbS particles are within the nanoscale.

A gas sensing performance of the sensor based on PbS/CdS heterostructures is highly depends on the operating temperature due to related adsorption–desorption property of the gas on the sensing material. The operating temperature is one of important sensing properties for a gas sensor and a low operating temperature such as room temperature is preferable for its practical applications. Nevertheless, most reports on the NH_3 sensors are focused on the high temperature sensing applications [14–16].

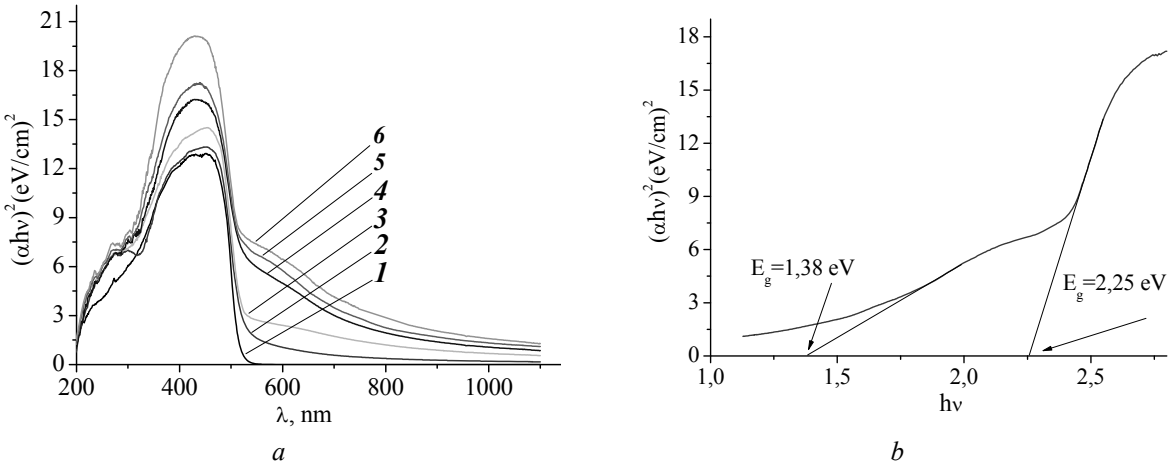

Fig. 2. UV-Vis absorption spectra of CdS nanorods and PbS/CdS heterostructures (plotted as the Kubelka-Munk function): *1* – CdS, *2* – 2.5 % PbS/CdS, *3* – 5 % PbS/CdS, *4* – 10 % PbS/CdS, *5* – 15 % PbS/CdS, *6* – 20 % PbS/CdS *(a),* optical band gap energy of heterostructure 15%PbS/CdS obtained by extrapolation to α = 0 *(b)*

The electrical resistance of the sensor was measured in presence and absence of examined gases. The values of electrical resistance of the sensor decrease quickly as soon as the NH_3 gas reacts with sensor material and then quickly returns to its initial values when refreshed with air, indicating a good repeatability and reversibility of the NH_3 sensor (Fig. 3).

For the semiconducting material, the following equation (5) was used to determine gas responses [17];

$$S(\%) = \frac{R_g - R_a}{R_a} \times 100 \quad (5)$$

where R_a is the resistance of the sensor in the fresh air and R_g is the resistance of the sensor in the presence of the test gas. Dynamic response transients of sensors are shown in Fig. 3. With increase in the PbS concentration in the PbS/CdS, the sensor's sensitivity increases, the reaction rate of the sensor increases too.

The semiconductor gas sensing mechanism is based on reactions between gas molecules and the surface of the material, which cause changes in the material resistance due to a charge transfer between the adsorbate and the adsorbent. The mobile oxygen on the semiconductor surface acts as the selective site in gas adsorption.

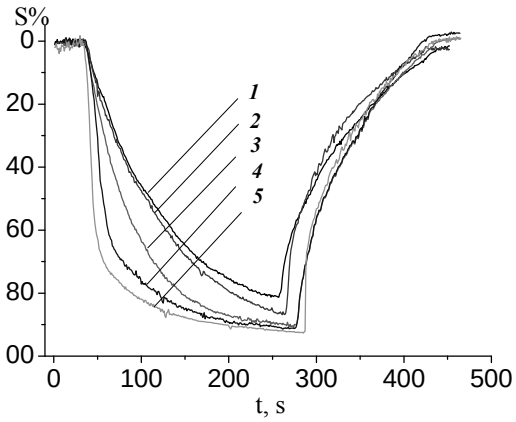

Fig. 3. Plot of gas response (%) versus time (s) for the PbS/CdS sensor device at a fixed voltage (0.5 V): *1* – 2.5 % PbS/CdS, *2* – 5 % PbS/CdS, *3* – 10 % PbS/CdS, *4* – 15 % PbS/CdS and *5* – 20 % PbS/CdS

When the sensor material is exposed to vapors of ammonia, the superficial reactions of NH_3 molecules with the oxygen species caused more electrons to return to the conduction band because ammonia acting as the electron donor. The surface reactions between the NH_3 and the sensor material can be described as follows [18–21]:

$O_2(gas) \leftrightarrow O_2(ads)$

$O_2(ads) + e^- \rightarrow O_2^-(ads)$

$O_2^-(ads) + e^- \rightarrow 2O^-(ads)$

$NH_3(gas) = NH_3(ads)$

$2NH_3(ads) + 3O^-(ads) \rightarrow N_2 + 3H_2O + 3e^-$

$2NH_3(ads) + 5O^-(ads) \leftrightarrow 3H_2O + 2NO_2 + 5e^-$

$4NO + 2NH_3 \rightarrow 2N_2 + N_2O + 3H_2O$

$NO + 1/2O_2(gas) \leftrightarrow NO_2$

$NO_2 + e^- \leftrightarrow NO_2^-(ads)$

$NO_2 + 1/2\ O_2(gas) + e^- \leftrightarrow NO_3^-(ads)$

where $O^-(ads)$, $NO_2^-(ads)$, and $NO_3^-(ads)$ represent negatively charged chemisorbed species, and e^- free electrons available for electrical conduction. The relations means that when the sensor is exposed to NH_3 containing gas, electrons trapped by the adsorptive states will be released, leading to a decrease in sensor resistance, as experimentally observed (Fig. 3).

When the pristine CdS is used as a sensor, a very slow recovery after NH_3 adsorption is observed. Resistance for the CdS sample is more than an order less in magnitude than that of the heterostructure PbS/CdS (Fig. 4).

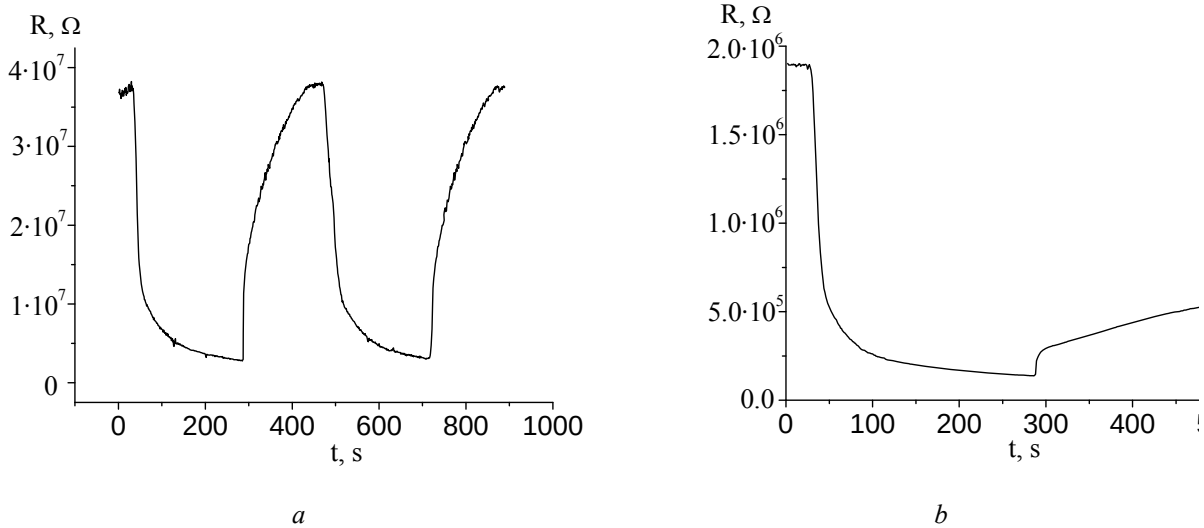

a *b*

Fig. 4. Dynamic response transients of sensors based on nanostructure 20 % PbS/CdS (two cycles) (*a*) and CdS (*b*) to NH_3 at room temperature

CONCLUSIONS

A simple chemical approach was used to deposit a PbS nanoparticles on the surface of CdS nanorods. Inclusion of Pb ions into CdS matrix improves the semiconductor sensing properties significantly. The sensors based on PbS/CdS heterostructures have better sensing response and recovery time when compared with the CdS-based sensor. Gas sensor based on nanoparticles PbS/CdS demonstrates an excellent sensitivity, rapid response/recovery time towards NH_3 gas at the room temperature.

Газовий датчик NH_3 на основі гетероструктур PbS/CdS, що працює в умовах кімнатної температури

С.Л. Прокопенко, Г.М. Гуня, С.М. Махно, П.П. Горбик

Інститут хімії поверхні ім. О.О. Чуйка Національної академії наук України
вул. Генерала Наумова, 17, Київ, 03164, Україна, sprokop@yandex.ru

З метою розробки датчиків, які можуть виявити шкідливі гази при кімнатній температурі, були синтезовані напівпровідникові гетероструктури PbS/CdS на основі наностржнів CdS. Використано метод іонного заміщення для нанесення наночастинок PbS на поверхню наностржнів CdS, для отримання великої площі поверхні гетеропереходу. Досліджено їх морфологія, оптичні властивості та характеристики датчика NH_3. Показано, що при збільшенні кількості PbS на поверхні CdS з 2.5 до 20 % швидкість відгуку датчика збільшується в 1.7 рази.

Ключові слова: *датчик, гетероструктури PbS/CdS, амоніак, наностржні*

Газовый датчик NH_3 на основе гетероструктур PbS/CdS, работающий в условиях комнатной температуры

С.Л. Прокопенко, Г.М. Гуня, С.Н. Махно, П.П. Горбик

Институт химии поверхности им. А.А. Чуйко Национальной академии наук Украины
ул. Генерала Наумова, 17, Киев, 03164, Украина, sprokop@yandex.ru

С целью разработки датчиков, которые могут обнаружить вредные газы при комнатной температуре, были синтезированы полупроводниковые гетероструктуры PbS/CdS на основе наностержней CdS. Использован метод ионного замещения для нанесения наночастиц PbS на поверхность наностержней CdS, для получения большой площади поверхности гетероперехода. Исследованы их морфология, оптические свойства и характеристики датчика NH_3. Показано, что при увеличении количества PbS на поверхности CdS с 2.5 до 20 % скорость отклика датчика увеличивается в 1.7 раза.

Ключевые слова: *датчик, гетероструктуры PbS/CdS, аммиак, наностержни*

REFERENCES

1. Erisman J.W., Sutton M.A., Galloway J., Klimont Z., Winiwarter W. How a century of ammonia synthesis changed the world. *Nat. Geosci*. 2008. **1**: 636.
2. Durbin T.D., Wilson R.D., Norbeck J.M., Miller J.W., Huai T., Rhee S.H. Estimates of the emission rates of ammonia from light-duty vehicles using standard chassis dynamometer test cycles. *Atmos. Environ*. 2002. **36**(9): 1475.
3. Tang Y.L., Li Z.J., Ma J.Y., Guo Y.J., Fu Y.Q., Zu X.T. Ammonia gas sensors based on ZnO/SiO_2 bi-layer nanofilms on ST-cut quartz surface acoustic wave devices. *Sens. Actuators, B*. 2014. **201**: 114.
4. Ament W., Huizenga J.R., Kort E., Mark T.W. van der, Grevink R.G., Verkerke G.J. Respiratory ammonia output and blood ammonia concentration during incremental exercise. *Int. J. Sports Med.* 1999. **20**(2): 71.
5. Wang S.Y., Ma J.Y., Li Z.J., Su H.Q., Alkurd N.R., Zhou W.L., Wang L., Du B., Tang Y.L., Ao D.Y., Zhang S.C., Yu Q.K., Zu Xiao-Tao Surface acoustic wave ammonia sensor based on ZnO/SiO_2 composite film. *J. Hazard. Mater*. 2015. **285**: 368.
6. Kim I.D., Rothschild A., Tuller H.L. Advances and new directions in gas-sensing devices. *Acta. Mater*. 2013. **61**(3): 974.
7. Comini E., Baratto C., Concina I., Faglia G., Falasconi M., Ferroni M., Galstyan V., Gobbi E., Ponzoni A., Vomiero A., Zappa D., Sberveglieri V., Sberveglieri G. Metal oxide nanoscience and nanotechnology for chemical sensors. *Sens. Actuators, B*. 2013. **179**: 3.
8. Zhao Q., Hou L., Huang R., Li S. Surfactant-assisted growth and characterization of CdS nanorods. *Inorg. Chem. Commun*. 2003. **6**(12): 1459.
9. Zhou H. S., Honma I., Komiyama H., Haus J. W. Coated semiconductor nanoparticles; the cadmium sulfide/lead sulfide system's synthesis and properties. *J. Phys. Chem*. 1993. **97**(4): 895.
10. Zhou H. S., Sasahara H., Honma I., Komiyama H., Haus J. W. Coated semiconductor nanoparticles: the CdS/PbS system's photoluminescence properties. *Chem. Mater.* 1994. **6**(9): 1534.
11. Liu B., Chew C. H., Gan L. M., Xu G. Q., Li H. P., Lam Y. L., Kam C. H., Que W. X. Third-order nonlinear optical response in PbS-coated CdS nanocomposites. *J. Mater. Res.* 2001. **16**(06): 1644.
12. Yadav S.K., Jeevanandam P. Thermal decomposition approach for the synthesis of $CdS\text{-}TiO_2$ nanocomposites and their catalytic activity towards degradation of rhodamine B and reduction of Cr(VI). *Ceram Int.* 2015. **41**(2): 2160.
13. Schoolar R.B., Dixon J.R. Optical Constants of Lead Sulfide in the Fundamental Absorption Edge Region *Phys. Rev. A*. 1965. **137**(2): 667.
14. Balamurugan C., Lee D.-W. A selective NH_3 gas sensor based on mesoporous *p*-type NiV_2O_6 semiconducting nanorods synthesized using solution method. *Sens. Actuators B*. 2014. **192**: 414.
15. Modafferi V., Panzera G., Donato A., Antonucci P.L., Cannilla C., Donato N., Spadaro D., Neri G. Highly sensitive ammonia resistive sensor based on electrospun V_2O_5 fibers. *Sens. Actuators B.* 2012. **163**: 61.
16. Deng J.N., Zhang R., Wang L.L., Lou Z., Zhang T. Enhanced sensing performance of the Co_3O_4 hierarchical nanorods to NH_3 gas. *Sens. Actuators, B*. 2015. **209**: 449.
17. Morrison S.R., Madou M.J. *Chemical Sensing with Solid State Devices*. (London: Academic Press, 1989).
18. Pengfeng Guo, Haibo Pan Selectivity of Ti-doped In_2O_3 ceramics as an ammonia sensor. *Sens. Actuators B*. 2006. **114**: 762.
19. Mani G.K., Bosco J., Rayappan B. A highly selective room temperature ammonia sensor using spray deposited zinc oxide thin film. *Sens. Actuators B.* 2013. **183**: 459.
20. Tulliani J.-M., Cavalieri A., Musso S., Sardella E. Room temperature ammonia sensors based on zinc oxide and functionalized graphite and multi-walled carbon nanotubes. *Sens. Actuators B*. 2011. **152**: 144.
21. Takao Y., Miyazaki K., Shimizu Y., Egashira M. High ammonia sensitive semiconductor gas sensors with double-layer structure and interface electrodes. *J. Electrochem. Soc.* 1994. **141**: 1028.

Received 27.07.2016, accepted 06.02.2017